

Operating regime for a backward Raman laser amplifier in preformed plasma

Daniel S. Clark^{a)} and Nathaniel J. Fisch^{b)}

Plasma Physics Laboratory, Princeton University, P.O. Box 451, Princeton, New Jersey 08543

(Received 28 January 2003; accepted 16 May 2003)

A critical issue in the generation of ultraintense, ultrashort laser pulses by backward Raman scattering in plasma is the stability of the pumping pulse to premature backscatter from thermal fluctuations in the preformed plasma. Malkin *et al.* [Phys. Rev. Lett. **84**, 1208 (2000)] demonstrated that density gradients may be used to detune the Raman resonance in such a way that backscatter of the pump from thermal noise can be stabilized while useful Raman amplification persists. Here plasma conditions for which the pump is stable to thermal Raman backscatter in a homogeneous plasma and the density gradients necessary to stabilize the pump for other plasma conditions are quantified. Other ancillary constraints on a Raman amplifier are also considered to determine a specific region in the T_e - n_e plane where Raman amplification is feasible. By determining an operability region, the degree of uncertainty in density or temperature tolerable for an experimental Raman amplifier is thus also identified. The fluid code F3D [R. L. Berger *et al.*, Phys. Plasmas **5**, 4337 (1998)], which includes the effects of thermal fluctuations, is used to verify these analytic estimates. © 2003 American Institute of Physics. [DOI: 10.1063/1.1590667]

I. INTRODUCTION

The recently proposed resonant backward Raman laser amplification scheme¹ utilizes the stimulated Raman backscatter in plasma of a long pumping laser pulse to amplify a short, frequency downshifted seed pulse. In the ultraintense regime, this scheme offers the possibility of focused intensities as high as 10^{25} W/cm² and pulse lengths of less than 100 fs for 1 μ m radiation. To reach these intensities, however, this technique relies on the propagation of the pumping pulse across a preformed plasma slab of approximately 1 cm in length prior to its interaction with the oppositely propagating seed. During this propagation, the pump will be subject to deleterious backward Raman scattering from thermal fluctuations in the plasma prior to interacting with the seed which could degrade or completely suppress the desired amplification. Reference 2 predicted that, due to the narrowing in time of the amplifying pulse, a nonlinear filtering effect of Raman amplification may be exploited by which a density gradient (or frequency chirp of the pump) may be introduced to detune and suppress Raman backscatter of the pump from thermal noise without suppressing the desired amplification of the seed pulse.

The problem of stability of laser pulses to nonlinear decay when propagating through plasmas is central to research in laser-driven inertial confinement fusion and has been extensively studied.^{3,4} Specifically, Mounaix *et al.*⁵ considered the problem of the propagation of a laser pulse of finite duration across a finite length uniform plasma subject to Brillouin backscatter from thermal noise. Successful comparison of their results with experiments were subsequently made.⁶ These calculations may be readily adapted to the case

of the space-time evolution of Raman backscatter, and comparisons with experiments have also been successful for such a case.⁷ Likewise, the subject of the influence of plasma inhomogeneities on backscattering has also long been studied in the context of inertial confinement fusion. Particular attention has been given to regimes of absolute or convective growth and to linear saturation levels for both bounded and infinite plasmas.⁸

This paper quantifies the plasma conditions as well as the steepness of any linear density gradient needed to stabilize the pump in a backward Raman amplifier. The work of Mounaix *et al.* is used, together with the results of Rosenbluth *et al.*⁹ and others, to derive analytic estimates of the specific constraints placed on the plasma conditions for stable pump propagation relevant to Raman amplification. These estimates are then compared with the results of fluid simulations which include the effects of thermal plasma noise. Other constraints on the plasma conditions are also considered. The combination of these constraints is then visualized as a region of operability for Raman amplification in the plane of plasma density and temperature. Since the plasma conditions in any experimental realization cannot be perfectly controlled, the parameter space is surveyed to determine in what regions Raman amplification is feasible as opposed to identifying any single optimal point. For pump durations of ~ 10 ps, Brillouin backscatter from thermal noise, while possible, is a secondary issue and is not considered here.

This paper is organized as follows. Section II describes the modeling of the space-time evolution of backscatter for a finite length homogeneous plasma and formulates these results as constraints on a Raman amplifier. Section III extends these results to the case of weakly inhomogeneous plasmas. Section IV describes several additional constraints

^{a)}Electronic mail: dclark@pppl.gov

^{b)}Electronic mail: fisch@pppl.gov

which apply to Raman amplification. Section V compares the results of the analytic estimates with a series of numerical simulations, and Sec. VI summarizes and concludes.

II. CONSTRAINTS DUE TO THERMAL NOISE IN HOMOGENEOUS PLASMAS

This section addresses the limitations on plasma density and temperature in a Raman amplifier due to backscatter of the pump from thermal fluctuations in the plasma medium in the absence of density gradients. For a uniform plasma, the effect of premature backscatter of the pump from noise may be estimated using the theory developed by Mounaix *et al.*⁵ Specifically, Ref. 5 considers the problem of the propagation of a square laser pulse across a plasma of length L in the presence of thermal fluctuations from the time of the pulse entering the plasma ($t=0$) to times $t>L/c$. The duration of the pulse is taken to be at least the time $2L/c$ of interest for the pump in a Raman amplifier. In the linear regime of the backscatter instability (when depletion of the pump is negligible, i.e., $a_1 = \text{const}$), the time evolution of the laser pulse, including a source of thermal Langmuir waves, is governed by the linearized three-wave equations,

$$\begin{aligned} (\partial_t + c \partial_x) a_2 &= \gamma_R a_3^*, \\ (\partial_t - \nu_3) a_3 &= \gamma_R a_2^* + S_3. \end{aligned} \quad (1)$$

Here $a_{1,2} \doteq |e| \langle A_{1,2} \rangle / m_e c^2$ are the normalized envelopes of the incident and scattered laser field vector potentials, $a_3 \doteq |e| \langle E_3 \rangle / m_e c \sqrt{\omega \omega_{pe}}$ is the normalized envelope of the resonant Langmuir wave, and $\gamma_R \doteq \omega a_1 (n_e/n_c)^{1/4} / 2$ is the linear Raman growth rate for linearly polarized lasers. The plasma is tenuous and cold in the regime of interest ($n_e/n_c \ll 1$ and $v_{\text{osc}} \doteq c a \gg v_{te}$) so that $\omega_1 \approx \omega_2 \equiv \omega \gg \omega_3 \approx \omega_{pe}$ and advection of the Langmuir wave has been neglected for the moment, $\nu_3 \approx 0$. The damping of the light waves has also been neglected, while ν_3 is the damping rate of the Langmuir wave (typically dominated by Landau damping). The ‘‘standard decay regime’’ for which this envelope formulation is valid is also assumed. Since only the threshold of instability is of interest here, the laser envelopes $a_{2,3}$ will *a priori* be in the linear regime and Eqs. (1) will always be valid. Finally, $n_c \doteq m_e \omega^2 / 4\pi |e|^2$ is the critical density, and ω_{pe} the electron plasma frequency.

The fluctuating Langmuir source S_3 is a stochastic function of space and time. Following Mounaix *et al.*, for consistency with the thermal fluctuation level (in one dimension) at the resonant wave number in the absence of instability ($\gamma_R \equiv 0$), the statistics of S_3 are determined by

$$\begin{aligned} \langle S_3(x, t) \rangle &= 0, \\ \langle S_3(x, t) S_3(x', t') \rangle &= \Sigma_3 \delta(x - x') \delta(t - t'), \end{aligned} \quad (2)$$

where

$$\Sigma_3 \doteq \frac{\omega}{2\pi} \frac{k_3^2}{n_c} \frac{\nu_3}{\omega_{pe}} \frac{T_e}{m_e c^2}$$

and $\langle \dots \rangle$ denotes ensemble average. A thermal source of backscattered light S_2 should in principle be included in Eqs. (1); however, it can be shown that

$$\frac{\Sigma_2}{\Sigma_3} = \left(\frac{\nu_2}{\nu_3} \right) \left(\frac{\omega_3}{\omega_2} \right) \left(\frac{k_2}{k_3} \right)^2 \approx \frac{1}{4} \left(\frac{\omega_{pe}}{\omega} \right)^3 \frac{\nu_{ei}}{\nu_{ei} + \nu_L} \ll 1$$

for ν_{ei} and ν_L the collisional and Landau damping rates, respectively. The Langmuir wave source, then, clearly gives the dominant contribution to the backscatter.

The (approximate) initial and boundary conditions to be applied in solving Eqs. (1), as described by Mounaix *et al.*, are thermal equilibrium levels of $a_{2,3}$ at the leading edge of the pump (i.e., thermal equilibrium pertains in the plasma which the pump has not yet traversed) and thermal fluctuation levels of a_2 at $x=L$. These conditions also represent stochastic functions of time with statistical properties similar to those of Eqs. (2). The additional effect of the propagation of the pump across the plasma can be modeled by an effective time dependence of the linear growth rate $\gamma_R = \gamma_0 \Theta(x) \Theta(x - ct)$ with $\Theta(x)$ the Heaviside step function.

For each realization of S_3 , a Green’s function method may be used to calculate the time evolution of $a_{2,3}$. Using the known statistical properties of S_3 , then, the ensemble average backscatter reflectivity $\langle |a_2/a_1|^2 \rangle$ may be calculated. In particular, for the strong damping regime $\gamma_0/\nu_3 \ll 1$ applicable here, the dominant contribution to the backscatter is due to the volume source of Langmuir waves as opposed to the boundary conditions. The enhancement of the reflectivity over its thermal value is then given by

$$\frac{1}{a_1^2} \langle |\delta a_2(x, t)|^2 \rangle \approx \frac{1}{a_1^2} \left\langle \left| \int_0^L dx' \int_{L-x'/c}^t dt' g(x-x', t-t') S_3(x', t') \right|^2 \right\rangle \quad (3)$$

with

$$\begin{aligned} g(x, t) &\doteq \frac{\gamma_0}{c} \Theta(x) \Theta(ct - c) e^{-\nu_3(t-x/c)} \\ &\times I_0 \left(\frac{2\gamma_0}{c} \sqrt{x(ct-x)} \right). \end{aligned}$$

Using the large argument expansion of the Bessel function $I_0(x) \sim e^x / \sqrt{2\pi x}$, Mounaix *et al.* derive a *uniform* approximation (i.e., valid for both large and small gains) for the backscatter reflectivity;

$$\frac{1}{a_1^2} \langle |\delta a_2(x, t)|^2 \rangle \sim \frac{R_{\text{TS}} \exp(G) - 1}{G \sqrt{1 + \pi G}}.$$

Here $G \doteq 2\gamma_0^2 \ell(x, t) / c \nu_3$ and $R_{\text{TS}} \doteq \Sigma_3 G / 4c$ are the gain factor and the thermal Thomson reflectivity, and $\ell(x, t) \doteq \min[x, (ct+x-L)/2]$. Note that, for small gains ($G \ll 1$), the reflectivity reduces to the Thomson value, while for large gains ($G \gg 1$) it mimics the large-argument behavior of the Bessel function.

For Raman amplification, the amplification length over which the pump could be backscattered, L in the above formulas, is constrained by the modulational instability of the amplifying seed.²³ In particular, for the evolving π -pulse of a Raman amplifier, the modulation growth time of the seed gives $L = c T_{\text{amp}}$ with $T_{\text{amp}} \sim 4a_1^{-4/3} / \omega_{pe}$. Since, in this ge-

ometry, the pump enters the plasma from the left ($x=0$) and remains on for a time $2L/c$ so that the seed may continually absorb more pump energy as it propagates the entire length L , the greatest amount of backscatter during the amplification process will occur at $x=0$ and $t=2T_{\text{amp}}$. Using this conservative estimate of the amount of backscatter, an operating regime in the T_e-n_e plane is then defined by the condition,

$$\Lambda \geq \frac{1}{a_1^2} \langle |\delta a_2(x=0, t=2T_{\text{amp}})|^2 \rangle, \quad (4)$$

where Λ represents the maximum reflectivity judged to be tolerable for a stable amplifier, e.g., $\Lambda=0.1$.

III. CONSTRAINTS DUE TO THERMAL NOISE IN INHOMOGENEOUS PLASMAS

In the presence of a weak linear density gradient, the linearized envelope equations become⁹

$$\begin{aligned} (\partial_t + c \partial_x) a_2 &= \gamma_R a_3^* \exp\left(\frac{i}{2} \kappa' x^2\right), \\ (\partial_t - v_3/2) a_3 &= \gamma_R a_2^* \exp\left(\frac{i}{2} \kappa' x^2\right) + S_3, \end{aligned} \quad (5)$$

where $\kappa' \doteq \partial \Delta k / \partial x$ is the rate of detuning from exactly resonant three-wave coupling, $0 = \Delta k \doteq k_1 - k_2 - k_3$. For the case of the Raman interaction, the variation of the plasma frequency with x is the dominant detuning effect so that

$$v_3 \kappa' \approx \frac{\partial \omega_{pe}}{\partial x} \equiv \frac{\omega_{pe}}{2L_n}$$

with L_n the density scale-length and v_3 the Langmuir wave group velocity. It proves convenient²⁴ to quantify this detuning in terms of the small dimensionless parameter,

$$q \doteq \frac{c \omega_{pe}}{4 \gamma_0^2 L_n} \equiv \frac{c v_3 \kappa'}{2 \gamma_0^2} \ll 1.$$

When assessing the lowest order effect of spatial detuning of the Raman resonance on the stability of the pump, it is no longer valid to neglect completely the group velocity of the Langmuir wave v_3 relative to that of the light waves. Indeed, without including the lowest order contribution of v_3 , the Green's function approach to calculating the backscatter reflectivity yields precisely the result found for a homogeneous plasma, i.e., no stabilizing effect is found. A simple substitution into Eq. (3) of the transformation found by Reiman¹⁰ for converting the detuned equations [Eqs. (5)] back to the homogeneous medium equations [Eqs. (1)], shows this directly when $v_3=0$. Physically, this is merely the result of the equivalence of the Langmuir wave having zero group velocity and being nondispersive ($v_3=0 \Leftrightarrow \partial \omega_3 / \partial k = 0$). Since ω_3 would not depend on k_3 in this case, the wave vector of the Langmuir wave may always adjust to "follow" the resonance condition as the density (and hence wave vectors of the light waves) changes with the result that no net detuning occurs and no stabilization is found. Mathematically, the Green's function given in Ref. 9 for linear wave coupling in an inhomogeneous plasma may be applied,

but the limit of $v_3 \rightarrow 0$ may be taken only if simultaneously $\kappa' \rightarrow \infty$ in such a way that $v_3 \kappa'$ is kept finite. The amplitude found for the backscatter does in fact only depend on v_3 through the combination $v_3 \kappa'$. Interestingly, the result used below for the backscatter Green's function [Eq. (6)] in the case of a density gradient detuning and the limit $v_3 \rightarrow 0$ (i.e., a detuning in wavelength) is effectively identical to the Green's function found by Ref. 2 for the case of a detuning in frequency when $v_3 \equiv 0$.

It should also be noted that, in the limit $v_3 \rightarrow 0$, the plasma inhomogeneity is the dominating effect over the finite plasma extent. The use of the infinite medium Green's function [Eq. (6)] is then a valid approximation to this order in v_3 .¹¹ Further, neglecting the propagation of the Langmuir wave will remain a valid approximation only for times $t \ll 2/v_3 \sqrt{\kappa'}$, i.e., so long as the Langmuir wave does not propagate out of the region of resonance. Using $v_3 \approx 3 v_{te}^2 k_3 / \omega_3$ and $v_3 \kappa' = 2 \gamma_0^2 q / c$, validity up to times $t \sim T_{\text{amp}} \sim 4 a_1^{-4/3} / \omega_{pe}$ then requires

$$q \ll \frac{4}{3} \left(\frac{n_e}{n_c}\right)^{-1} \left(\frac{T_e}{m_e c^2}\right) a_1^{-2/3}.$$

For typical parameters, this again amounts to $q \ll 1$.

As shown in Ref. 9, the Green's function for the inhomogeneous case is given by (again neglecting damping of the light wave and keeping only the combination $v_3 \kappa'$)

$$\begin{aligned} g(x, t) &= \frac{\gamma_0}{\pi c} \sinh\left(\frac{\pi}{2q}\right) e^{-v_3(t-x/c) + iq \eta} \\ &\times \int_0^1 \frac{dz}{z} \left(\frac{z}{1-z}\right)^{i/2q} e^{-2iq \eta z}, \end{aligned} \quad (6)$$

where $\eta \doteq \gamma_0^2 x(ct-x)/c^2$.²⁵ A convenient form for this solution is found by identifying Eq. (6) as an integral representation of a confluent hypergeometric function,^{12,26} namely,

$$\begin{aligned} g(x, t) &= i \frac{2 \gamma_0}{c} \sinh\left(\frac{\pi}{2q}\right) e^{-v_3(t-x/c) + iq \eta - \pi/2q} \\ &\times {}_1F_1\left(\frac{i}{2q}, 1; -2iq \eta\right). \end{aligned}$$

For early times, $q \eta \ll 1$, ${}_1F_1$ may be expanded in a series of modified Bessel functions,¹³

$${}_1F_1\left(\frac{i}{2q}, 1; -2iq \eta\right) = I_0(2\sqrt{\eta}) + iq \eta I_2(2\sqrt{\eta}) + \dots \quad (7)$$

showing that the evolution in the inhomogeneous case is only slightly perturbed from that of the homogeneous case. For late times, $q \eta \gg 1$, the large argument expansion of ${}_1F_1$ yields¹⁴

$${}_1F_1\left(\frac{i}{2q}, 1; -2iq \eta\right) \sim \frac{e^{\pi/2|q| + 4q^2/3}}{\sqrt{2\pi} \sqrt{1 + 1/4q^2}} e^{i\phi} \quad (8)$$

indicating saturation of the instability. ϕ is a purely real phase factor. The condition $q \eta \sim 1$ identifies the onset of saturation for any point x . Since, for any point, the instability first grows in a form similar to the homogeneous case and then saturates at a level given by Eq. (8), an approximate

representation of the Green's function is simply to take the minimum of Eqs. (7) and (8). Repeating the calculation outlined above in Eq. (3) with this approximate Green's function and neglecting any modifications to the statistical properties of S_3 due to the weak gradient leads to

$$\frac{1}{a_1^2} \langle |a_2(x,t)|^2 \rangle \sim R_{TS} \min \left[\frac{\exp(\pi/|q|)}{\pi/|q|}, \frac{\exp(G)-1}{G\sqrt{1+\pi G}} \right]. \quad (9)$$

Again, an operating regime is defined by the analogue of Eq. (4).

It should be noted that a similar result has been found by Mounaix *et al.*¹⁵ The calculation of Ref. 15, however, is of the steady-state reflectivity due to backscatter in an inhomogeneous plasma in the strong damping limit. To assess the stability of the pumping laser pulse to backscatter from noise in a Raman amplifier, the maximum reflectivity of the noisy plasma must be found over the length of the amplifier plasma and in general over the total time of amplification, i.e., the problem is temporal as well as spatial. Mounaix *et al.* note that in the strong damping limit, a steady-state reflectivity may rapidly be reached; however, on the time scales (~ 50 ps) and for parameters of interest to Raman amplification, this is not *a priori* the case as evidenced by the two-part structure of Figs. 1–4 discussed below. The evolution in time of the linearly growing backscatter of the pump from noise, and not merely the saturated gain from an arbitrarily long laser pulse, must then be followed.

Appropriately, the saturated limit of Eq. (9) agrees with the steady-state result of Ref. 15 in the strongly inhomogeneous limit, i.e., when the effect of spectral gain narrowing is negligible. In the course of deriving the approximate form of Eq. (9) from the exact Green's function for the inhomogeneous problem, the effect of gain narrowing has been neglected. For the sake of conservatively assessing the operating regime of a Raman amplifier, this neglect of the stabilizing effect of gain narrowing is an appropriate approximation. Interestingly, the transformation $x \rightarrow \mathcal{L}(x,t)$ can be used to connect the steady-state result of Ref. 15 with the time-dependent result of Eq. (9) provided again the effect of gain narrowing is neglected. Here, the $\min(\cdot)$ function appearing in Eq. (9) and arising from the large and small argument limits of the hypergeometric function is the analogue of the $\tan^{-1}(\cdot)$ appearing in the reflectivity calculated by Ref. 15.

IV. OTHER CONSTRAINTS ON RAMAN AMPLIFICATION

In addition to instability of the pump to thermal noise, several other factors limit the operating regime of a Raman amplifier. To calculate these constraints, the very weak density gradients considered above have been neglected, so that only the simpler uniform plasma results will be used.

First, the plasma conditions must be such that the pump is not excessively absorbed due to inverse-Bremsstrahlung while propagating across the plasma. Again, choosing $\Lambda = 0.1$ as a threshold for excessive absorption, the inverse-Bremsstrahlung constraint may be written

$$\frac{1}{2} \nu_{IB} T_{\text{amp}} \leq -\ln(1 - \Lambda^{1/2})$$

with ν_{IB} the inverse-Bremsstrahlung absorption coefficient.¹⁶ Note that, for simplicity this effect of damping of the pump beam has been neglected in the calculation of pump stability from Secs. II and III. This omission will be commented on in Sec. V.

Secondly, the necessity of avoiding breaking of the backscatter driven Langmuir wave and subsequent incomplete depletion of the pump imposes a lower bound on the allowable plasma electron density. Using the Manley–Rowe relations to find $a_3^{\text{max}} \sim a_1$ and the wave-breaking criteria for a cold plasma $\omega_p > \omega_b \doteq \sqrt{|e|k_3 E_3/m_e}$ (Ref. 4) leads to

$$n_e \geq n_c (4a_1)^{4/3}.$$

Note that the constraint here applies to breaking of the Langmuir wave driven by backscatter in the field of the seed and not thermal backscatter of the pump. As such, the Langmuir wave is growing in the transient, nonlinear regime, during which the pump and seed amplitudes (to which the Langmuir wave amplitude is coupled) are rapidly evolving, and is not constrained to $a_3^{\text{max}} \sim (\gamma_0/\nu_3)a_2 \ll a_2$ as might be expected of the strongly damped regime.⁵ Given that the seed pulse is short compared to the damping length of the Langmuir wave and of high amplitude, the transient Langmuir wave is rapidly driven to amplitudes comparable to the Manley–Rowe value within the seed even for $\nu_3 \gg \gamma_0$. This amplitude is confirmed by the plots in Figs. 5 and 6. Outside of the rapidly amplifying seed pulse, enslavement of the Langmuir wave to the backscatter wave in the strong damping regime applies. The amplitude in this region, however, does not determine the wave breaking limitation for the amplifier.

Thirdly, excessive Landau damping of the driven Langmuir wave which would also result in incomplete depletion of the pump should be avoided. An approximate constraint is

$$k_3 \lambda_{De} \leq \frac{1}{2}.$$

There is an added constraint to the operation of a Raman amplifier due to the possibility of forming broad nonlinear precursor pulses in place of the compressing π -pulse on which the amplification is based.¹⁷ Since this is an effect governed by the initial shape of the seed pulse and not controlled by the ambient plasma conditions, it cannot be addressed by the formalism used here.

Taken together, for a particular incident pump intensity and laser wavelength, the constraints given above and in Secs. II and III demarcate a specific region in plasma density and temperature for which Raman amplification should be feasible (Figs. 1–4). Note that if, in a particular experimental setup, a plasma length different from the optimal scaling of L_{amp} above were used, the results of Figs. 1–4 would be modified accordingly.

V. COMPARISON WITH FLUID CODE SIMULATIONS

The constraints presented above on the regime of operation for a backward Raman amplifier have been verified by comparison with a series of simulations using the F3D code. The details of the numerics of F3D and the noise model used

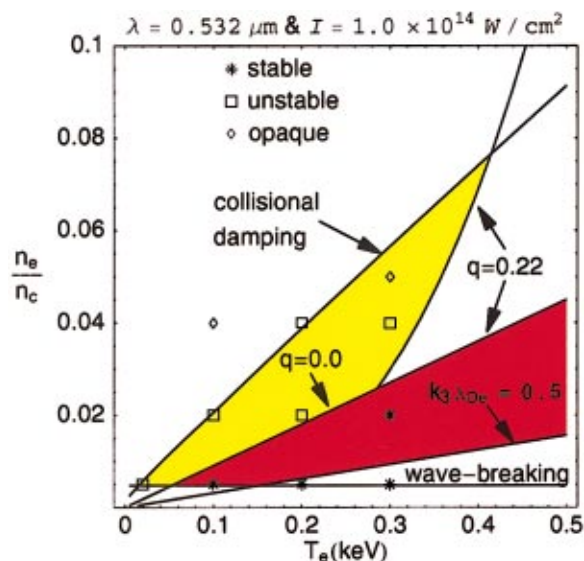


FIG. 1. (Color) Comparison of analytic estimates of constraints for stable Raman amplification with results of F3D simulations for $\lambda = 0.532 \mu\text{m}$ and $I = 1.0 \times 10^{14} \text{ W/cm}^2$. For $q = 0.0$ the region suitable for Raman amplification is shaded red, and for $q = 0.22$ both the red and yellow regions become suitable. The results of F3D simulations with $q = 0.0$ are represented by the symbols. When rerun with $q = 0.15 - 0.2$, all of the simulations which were unstable for $q = 0.0$ were stabilized.

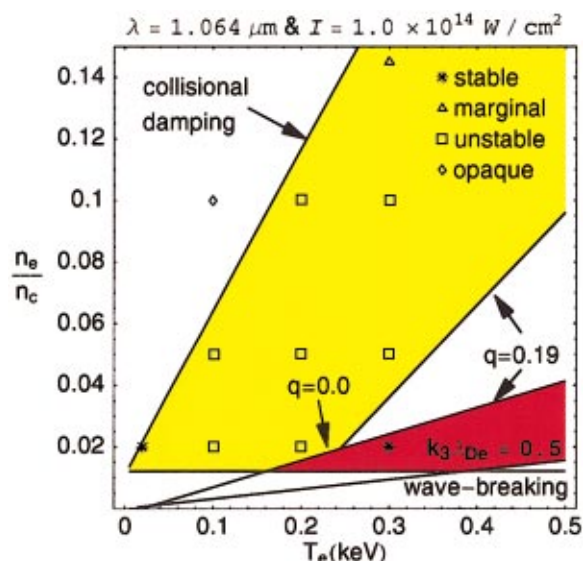


FIG. 3. (Color) Comparison of analytic estimates of constraints for stable Raman amplification with results of F3D simulations for $\lambda = 1.064 \mu\text{m}$ and $I = 1.0 \times 10^{14} \text{ W/cm}^2$. With $q = 0.0$, the red region is suitable for amplification, while for $q = 0.19$ both the red and yellow regions are suitable. The results of F3D simulations with $q = 0.0$ are represented by the symbols. When rerun with $q = 0.15 - 0.2$, all of the simulations which were unstable for $q = 0.0$ were stabilized.

in the code are described at length in Ref. 18. For each of four representative combinations of laser wavelengths and intensities ($\lambda = 0.532 \mu\text{m}$ and $1.064 \mu\text{m}$; $I = 1.0 \times 10^{14} \text{ W/cm}^2$ and $2.0 \times 10^{14} \text{ W/cm}^2$), a sequence of simulations was run to span the relevant portion of the electron density and temperature plane for helium plasmas. With each choice of density and temperature, the length of the simula-

tion was adjusted to correspond to the growth length for the modulational instability of the amplifying seed and cases were run with both uniform density profiles and a series of increasing density gradients (corresponding typically to $q = 0.0, 0.05, 0.1, 0.15, 0.2$, and 0.25).

While the primary focus here is the stability of the pump, seed pulses were also launched in the simulations to

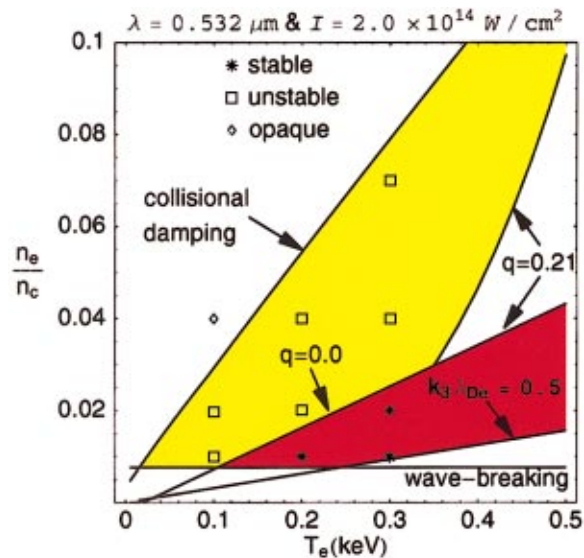


FIG. 2. (Color) Comparison of analytic estimates of constraints for stable Raman amplification with results of F3D simulations for $\lambda = 0.532 \mu\text{m}$ and $I = 2.0 \times 10^{14} \text{ W/cm}^2$. As in Fig. 1, with $q = 0.0$, the red region is suitable for amplification, while for $q = 0.21$ both the red and yellow regions are suitable. The results of F3D simulations with $q = 0.0$ are represented by the symbols. When rerun with $q = 0.15 - 0.2$, all of the simulations which were unstable for $q = 0.0$ were stabilized.

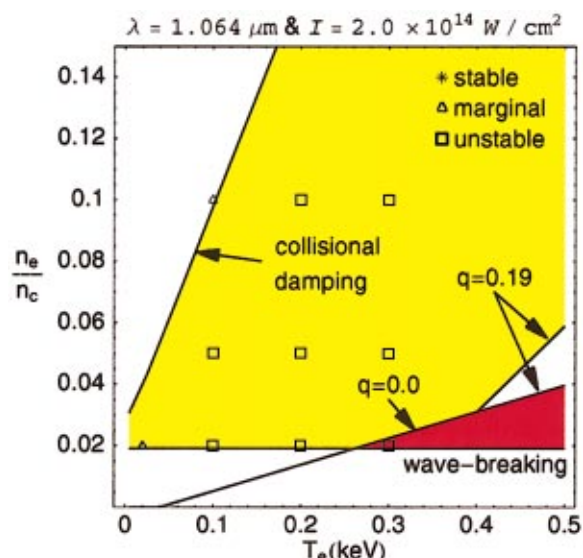


FIG. 4. (Color) Comparison of analytic estimates of constraints for stable Raman amplification with results of F3D simulations for $\lambda = 1.064 \mu\text{m}$ and $I = 2.0 \times 10^{14} \text{ W/cm}^2$. With $q = 0.0$, the red region is suitable for amplification, while for $q = 0.19$ both the red and yellow regions are suitable. The results of F3D simulations with $q = 0.0$ are represented by the symbols. When rerun with $q = 0.15 - 0.2$, all of the simulations which were unstable for $q = 0.0$ were stabilized.

gauge the effect on net amplification by varying temperatures and densities. The seed pulses were in all cases launched exactly when the pump had completely crossed the plasma from the opposite side and were given an amplitude equal to that of the pump and a trapezoidal shape in time with a 0.2 ps flat-top and 0.021 ps “risers.” Since the π -pulse is an attractor solution of the three-wave equations, provided the initial seed is sufficiently intense and sharp to reach this attractor, its actual shape should have little influence on the ultimate degree of amplification.

To compare easily with the above analytic results and for speed of computation, all simulations were run in only one dimension. Since direct backscatter is the fastest growing of the Raman interactions, no essential modifications of the physics are expected by including more than one dimension, at least as concerns the issue of amplifier stability to pump depletion by Raman backscatter from thermal noise. The effects of inverse-Bremsstrahlung of the laser fields and Landau damping of the Langmuir wave were also included in the simulations. A model for Langmuir wave breaking is not currently available in F3D.

The comparison of the analytic estimates and the numerical results is summarized by Figs. 1–4. The labeled curves correspond to the constraints discussed above: Above the curve labeled “collisional damping,” more than 10% attenuation of the pump from inverse-Bremsstrahlung should be expected. Below the line labeled “wave-breaking,” the driven Langmuir wave can be expected to break, preventing complete pump depletion and hence degrading the amplification efficiency. The curve label “ $k_3\lambda_{De}=0.5$ ” represents an approximate boundary beyond which Landau damping of the Langmuir wave should become strong. The curves labeled “ $q=\dots$ ” are the boundaries above or to the right of which more than 10% backscatter of the pump intensity can be expected for the corresponding density gradient. That is, for $q\neq 0.0$, only points below or to the left of the corresponding curve would be stable to thermal noise. Note that the curves labeled for $q\neq 0.0$ include part of the $q=0.0$ curve before curving steeply upward in n_e . This merely reflects the minimum function appearing in Eq. (9): for sufficiently high temperatures at a given density, the development of the instability is as if the plasma were uniform, while below some threshold temperature the instability saturates at a level dependent on q . With increasing values of q , this “turning point” moves progressively further to the right (i.e., to higher temperatures) and renders a larger portion of the T_e - n_e plane stable to pump backscatter—as can be expected physically. The red area denotes the stable domain for $q=0.0$, i.e., a homogeneous plasma. For the corresponding $q>0.0$, this stable domain is extended to include the red and yellow areas. The simulation results are represented by the symbols (*, Δ , \square , \diamond) and were judged stable, marginal, unstable, or opaque, respectively, on the criteria of 10% backscatter of the pump from thermal noise in a homogeneous plasma or 10% attenuation of the pump due to inverse-Bremsstrahlung. The results of simulations with $q\neq 0.0$ are discussed below.

The results of the simulations are seen to be in generally good agreement with the analytic estimates. The points cor-

responding to ($T_e=20$ eV, $n_e=0.02n_c$) in Fig. 3 and ($T_e=20$ eV, $n_e=0.02n_c$) and ($T_e=100$ eV, $n_e=0.1n_c$) from Fig. 4, however, show stability or marginal stability when instability should be expected. This can be ascribed to the strong amounts of collisional damping experienced by the pump in these runs: since the backscatter of thermal noise is exponentially dependent on the amplitude of the pump, degradation of the pump by inverse-Bremsstrahlung can substantially reduce the growth of noise (an effect neglected in the analytic estimates) and render an otherwise stable point unstable. It should be noted that the vertical scale of Figs. 3 and 4 is increased from that of Figs. 1 and 2 since the effect of inverse-Bremsstrahlung is lessened for longer wavelengths and hence opens a larger area of parameter space for consideration. Also, the line representing $k_3\lambda_{De}=0.5$ has been omitted from Fig. 4 since it is always below the wave-breaking constraint for this range of temperatures.

As an example of the effects of noise on the pump, snapshots of the evolving laser field envelopes are shown in Fig. 5 for the simulation corresponding to the point ($T_e=200$ eV, $n_e=0.02n_c$) from Fig. 1—just beyond the instability boundary. Initially, the pump (shown in blue) propagates stably across the plasma from the left but by $t=33$ ps is strongly depleted by thermal backscatter, while the seed (shown in green) is only beginning to propagate through the plasma. Evidently, the stability boundary marked by $q=0.0$ in Fig. 1 represents a quite steep transition between stability and instability. In Fig. 6 is shown the result of an identical run but with a slight density gradient corresponding to $q=0.15$. The thermal noise (barely visible as the red Langmuir fluctuations for $t>33$ ps) is seen to be completely stabilized by the gradient, and the seed pulse is much more strongly amplified. Note, however, that, due to the density detuning, only $\sim 50\%$ of the pump energy is backscattered into the seed.

Generally, for uniform plasmas, the maximum amplification of the seed (i.e., optimal operating point for a Raman amplifier) occurs for the lowest T_e and n_e consistent with the constraints due to wave-breaking and thermal noise and is represented by the lower left corner of the shaded area in the figures. Respectively, this corresponds simply to reducing as much as possible the Landau damping of the driven Langmuir wave and lengthening as much as possible the growth time of the modulational instability of the seed. In particular, the point corresponding to ($T_e=100$ eV, $n_e=0.005n_c$) of Fig. 1 attained a seed amplitude 285 times that of the pump, namely 2.85×10^{16} W/cm².

For nonuniform plasmas, based on the analytic estimates above, $q\sim 0.2$ is sufficient to stabilize the pump across the entire region of the n_e - T_e plane shown in Figs. 1–4. That is, any operating point between the boundary where inverse-Bremsstrahlung of the pump becomes excessive and $T_e\sim 500$ eV should be feasible for amplification. For temperatures beyond 500 eV still larger density gradients would be needed to control thermal noise, though such points are already very far from the desirable regime for Raman amplification. From the simulations, $q=0.15$ – 0.2 proved sufficient to ensure stability for all of the temperature and density com-

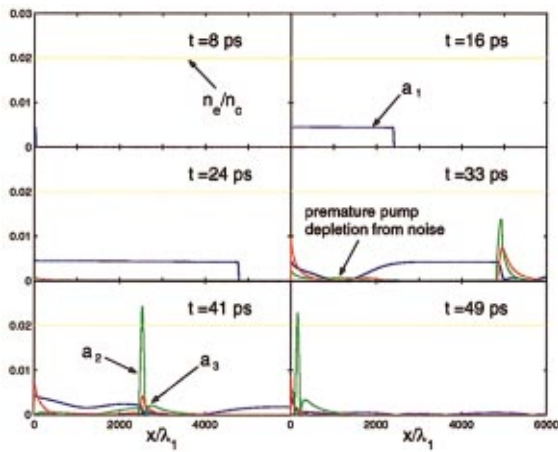


FIG. 5. (Color) Snapshots of laser field envelopes illustrating the effect of premature pump backscatter from thermal noise on Raman amplification when $\lambda = 0.532 \mu\text{m}$, $I = 1.0 \times 10^{14} \text{ W/cm}^2$, $T_e = 200 \text{ eV}$, $n_e = 0.02n_c$, and $q = 0.0$.

binations tried. Namely, when the simulations which were unstable for a homogeneous plasma (the open squares in Figs. 1–4) were rerun with inhomogeneous plasmas, the choice of $q = 0.15$ – 2.0 rendered them stable. By comparing with Figs. 1–4, this result is in good agreement with the analytical predictions.

It is evident from the figures that a stable regime exists for Raman amplification in this idealized model *even in the absence of density gradients*. However, the greatest amplification was obtained for the point ($T_e = 20 \text{ eV}$, $n_e = 0.005n_c$) with $q = 0.15$ in Fig. 1, namely a seed output intensity 390 times greater than the pump corresponding to $3.9 \times 10^{16} \text{ W/cm}^2$. This is a reflection of the fact that stability to thermal noise is governed most strongly by Landau damping of the Langmuir wave, i.e., the rate of growth of a given fluctuation is exponentially dependent on the Landau damping rate of the driven Langmuir wave. However, the useful Raman amplification is also dependent on the growth of the driven Langmuir wave, such that entering a regime of density and temperature where Landau damping is minimal but

where backscatter from thermal noise is controlled by a density gradient should be optimal. Clearly, too steep a density gradient will completely suppress the Raman resonance such that a balance must then be sought between minimizing Landau damping and not requiring an excessively strong gradient.

Note that the boundary for instability to thermal backscatter is to a good approximation merely a linear relationship between n_e/n_c and T_e . Again, this represents the importance of Landau damping in determining the stability to noise: for the case of Fig. 1, the boundary is roughly coincident with the line $k_3\lambda_{De} \approx 1/(2\sqrt{3})$. A simplification of Eq. (4) to represent this simple fact [namely, that the delineating value should be $1/(2\sqrt{3})$ as opposed to some other value], however, could not be found, and illustrates the importance of the initial thermal fluctuation levels in determining the ultimate stability of the pump.

VI. CONCLUSIONS

Many simplifications have been made in calculating the above constraints. While the approximation of a one-dimensional interaction should capture the dominant effects of direct Raman backscatter in determining the stability of the pump, two- or three-dimensional effects related to finite focusing widths and lengths and the proper overlap of pump and seed pulse may substantially degrade the efficiency of interaction from the simulation results presented above. The assumption of perfectly tailored density profiles (either perfectly square for the homogeneous case or with a precisely prescribed density gradient for the inhomogeneous case) is also unrealistic. Indeed, one of the greatest challenges in demonstrating Raman amplification experimentally may be in the production of adequately uniform plasmas. Finally, based on the results found in Sec. V, the interaction of attenuation of the pump by inverse-Bremsstrahlung and pump stability to thermal noise may not always be negligible.

In summary, the constraints on plasma parameters for the stability of the pump in a plasma-based backward Raman laser amplifier, as well as other ancillary constraints, have been quantified. The combination of these constraints has been visualized as a region in the plane of plasma density and temperature from which the most favorable regime for Raman amplification can be easily identified. Specific choices of wavelength and pump intensity have been used for illustration of these constraints, and agreement between the analytic estimates and numerical simulations has been demonstrated. It is evident that Landau damping of the driven Langmuir wave in the Raman interaction plays a crucial role in determining the stability of the pump. In particular, for $\lambda = 0.532 \mu\text{m}$ and $I = 1.0 \times 10^{14} \text{ W/cm}^2$, plasma densities and temperatures such that $k_e\lambda_{De} \geq 1/(2\sqrt{3})$ approximately determine a region of pump stability. Within this constraint, the lowest densities and temperatures consistent with avoiding the breaking of the driven Langmuir wave ($n_e \geq n_c(4a_1)^{4/3}$) provide optimal amplification since damping of the driven Langmuir wave and limitation by the modulational instability of the amplifying seed are then minimized. Outside of this constraint, density gradients cor-

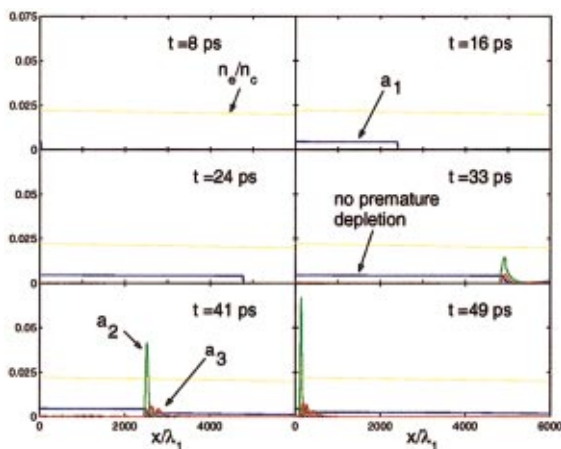


FIG. 6. (Color) Snapshots of laser field envelopes for the same parameters as Fig. 5 but with $q = 0.15$.

responding to $q \approx 0.2$ were found sufficient to stabilize the pump up to temperatures of $T_e \sim 500$ eV. The greatest amplification factor of 390 times in the seed intensity over the input pump intensity (corresponding to $I_{\text{out}} = 3.9 \times 10^{16}$ W/cm²) was observed for the case of a simulation with $\lambda = 0.532$ μm , $T_e = 20$ eV, $n_e = 0.005n_c$, and $q = 0.15$.

ACKNOWLEDGMENTS

The help of R. L. Berger in preparing simulations with F3D and on the general theory and modeling of backscatter from thermal noise is gratefully acknowledged. Many insightful comments were also received from the referee.

This work was supported by the U.S. Department of Energy Contract No. DE-AC02-76-CHO-3073 and the Defense Advanced Research Projects Agency (DARPA).

¹V. M. Malkin, G. Shvets, and N. J. Fisch, Phys. Rev. Lett. **82**, 4448 (1999).

²V. M. Malkin, G. Shvets, and N. J. Fisch, Phys. Rev. Lett. **84**, 1208 (2000).

³J. D. Lindl, *Inertial Confinement Fusion: The Quest for Ignition and Energy Gain Using Indirect Drive* (American Institute of Physics, New York, 1998).

⁴W. L. Kruer, *The Physics of Laser Plasma Interactions* (Addison-Wesley, New York, 1988).

⁵P. Mounaix, D. Pesme, W. Rozmus, and M. Casanova, Phys. Fluids B **5**, 3304 (1993).

⁶H. A. Baldis, D. M. Villeneuve, B. L. Fontaine *et al.*, Phys. Fluids B **5**, 3319 (1993).

⁷C. Rousseaux, G. Malka, J. L. Miquel *et al.*, Phys. Rev. Lett. **74**, 4655 (1995).

⁸K. Nishikawa and C. S. Liu, in *Advances in Plasma Physics* (Wiley, New York, 1976), Vol. 6, p. 3.

⁹M. N. Rosenbluth, R. B. White, and C. S. Liu, Phys. Rev. Lett. **31**, 1190 (1973).

¹⁰A. Reiman, Rev. Mod. Phys. **51**, 311 (1979).

¹¹D. Pesme, G. Laval, and R. Pellat, Phys. Rev. Lett. **31**, 203 (1973).

¹²J. Mathews and R. L. Walker, *Mathematical Methods of Physics* (Addison-Wesley, New York, 1970).

¹³M. Abramowitz and I. A. Stegun, *Handbook of Mathematical Functions* (Wiley, New York, 1984).

¹⁴N. N. Lebedev, *Special Functions and Their Applications* (Dover, New York, 1972).

¹⁵P. Mounaix, D. Pesme, and M. Casanova, Phys. Rev. E **55**, 4653 (1997).

¹⁶*NRL Plasma Formulary*, Naval Research Laboratory Publication NRL/PU/6790-00-426, edited by J. D. Hubac (U. S. GPO, Washington, D.C., 2000).

¹⁷Y. A. Tsidulko, V. M. Malkin, and N. J. Fisch, Phys. Rev. Lett. **88**, 235004 (2002).

¹⁸R. L. Berger, C. H. Still, E. A. Williams, and A. B. Langdon, Phys. Plasmas **5**, 4337 (1998).

¹⁹V. M. Malkin, Y. A. Tsidulko, and N. J. Fisch, Phys. Rev. Lett. **85**, 4068 (2000).

²⁰A. Bers, in *Handbook of Plasma Physics*, edited by M. N. Rosenbluth and R. Z. Sagdeev (North-Holland, New York, 1983), Vol. 1, p. 451.

²¹F. W. Chambers, Ph.D. thesis, Massachusetts Institute of Technology, 1975.

²²R. Lindberg and J. S. Wurtele (private communication, 2002).

²³As noted in Ref. 1, forward Raman scattering (FRS) of the amplified seed may also limit the amplification length. Since the growth times of FRS and modulational instabilities are roughly comparable in the regime of interest and since FRS may be stabilized by the introduction of a weak density gradient (Ref. 19) (as considered in Sec. III), for simplicity the amplification length is taken here to be constrained only by the modulational instability. Generalization to include the constraint of FRS, however, would be straightforward.

²⁴Chirping of the pump frequency would have an effect similar to that of a density gradient on the resonance. By properly defining q , the following results could also be applied to this case (Ref. 2).

²⁵References 20 and 21 have pointed out that there are many misprints/errors in Ref. 9. Though the essential results are correct, the supporting formulas must be used cautiously.

²⁶This result was first noticed by seeking a solution of Eqs. (5) explicitly in terms of η (Ref. 22).